

Analytical Methods

Accepted Manuscript



This is an *Accepted Manuscript*, which has been through the Royal Society of Chemistry peer review process and has been accepted for publication.

Accepted Manuscripts are published online shortly after acceptance, before technical editing, formatting and proof reading. Using this free service, authors can make their results available to the community, in citable form, before we publish the edited article. We will replace this *Accepted Manuscript* with the edited and formatted *Advance Article* as soon as it is available.

You can find more information about *Accepted Manuscripts* in the [Information for Authors](#).

Please note that technical editing may introduce minor changes to the text and/or graphics, which may alter content. The journal's standard [Terms & Conditions](#) and the [Ethical guidelines](#) still apply. In no event shall the Royal Society of Chemistry be held responsible for any errors or omissions in this *Accepted Manuscript* or any consequences arising from the use of any information it contains.

Assembly of Fe-pamoate porous complex on magnetic microspheres for extraction of sulfonamide antibiotics from environmental water samples

Huan Wang, Si-Yao Liu, Xiao-Jun Lv, Rui Ma, Zhi-Qi Zhang *

(Key Laboratory of Analytical Chemistry for Life Science of Shaanxi Province, School of Chemistry and Chemical Engineering, Shaanxi Normal University, Xi'an 710062, China)

Abstract

Unique ternary single core-double shell structured magnetic microspheres of $\text{Fe}_3\text{O}_4@\text{SiO}_2@\text{Fe-pamoate}$ were successfully fabricated via a step-by-step assembly strategy. The procedures involved initial pre-treatment of the silica-coated magnetic cores with carboxyl groups to functionalize the magnetic microspheres, and subsequent alternating treatments with Fe^{3+} and pamoic acid solutions for growth of Fe-pamoate complexes on the microsphere surface to form $\text{Fe}_3\text{O}_4@\text{SiO}_2@\text{Fe-pamoate}$ magnetic microspheres. Characterization using various techniques demonstrated that the microspheres were porous, thermally stable, and possessed a single core-double shell sandwich structure. The as-synthesized materials possessed bifunctional character derived from the magnetic properties of the Fe_3O_4 nanoparticles and the high porosity of Fe-pamoate, making them excellent candidates as adsorbents for the magnetic enrichment of trace analytes. The potential applicability of the microspheres was demonstrated by preconcentrating sulfonamide antibiotics from environmental water samples prior to high-performance liquid chromatography analysis. The method combined enrichment with high-performance liquid chromatography had higher precision (relative standard deviations 1.4–12.3%), lower detection limits (0.08–0.12 ng mL^{-1}), and good linearity (correlation coefficients higher than 0.9947) for investigated five sulfonamide antibiotics. Average recoveries at three spiked levels were in the range of 86.3 to 99.7% with relative standard deviations below 12.3%.

Keywords: Magnetic single core-double shell microsphere, Fe-pamoate complex, sulfonamide antibiotics, extraction, high performance liquid chromatography.

* Corresponding author. Tel.: +86 29 81530792; fax: +86 29 81530792.
E-mail address: zqzhang@snnu.edu.cn (Z.-Q. Zhang).

1. Introduction

Significant research has been devoted to development of magnetic particles and improvement of their applications in various areas [1]. Iron oxides have received the most attention, because of their strong magnetic responsiveness and biocompatibility [2]. However, unmodified Fe_3O_4 particles aggregate readily and do not adsorb analytes effectively. Therefore, modification of these Fe_3O_4 particles with various functional groups is a strategy commonly employed to prevent aggregation and extend the range of their applications. Lee and coworkers prepared antibiofouling polymer-coated superparamagnetic iron oxide nanoparticles for in vivo cancer imaging [3]. Arruebo et al. utilized magnetic silica-based materials for drug-delivery applications [4]. Deng and coworkers synthesized core/shell colloidal magnetic zeolite microspheres for the immobilization of trypsin [5]. Wang et al. formed a graphene-coated magnetic nanocomposite for the enrichment of fourteen pesticides in tomato and rape samples [6]. Various synthesis strategies have been developed for the preparation of magnetic materials. Carbon coated Fe_3O_4 magnetic particles, carbon@ Fe_3O_4 , have been synthesized by hydrothermal reaction treatment [7,8]. Novel core@shell-structured magnetic zeolite microspheres were synthesized by using a combination of seed coating and vapour-phase transport [4]. Porous microspheres with a magnetic core and a tunable metal-organic coordination polymer shell were successfully fabricated by utilizing a versatile step-by-step assembly strategy [9–10].

Magnetic metal-organic coordination polymers, which are composite materials composed of iron oxide and metal-organic coordination polymers, have been used as magnetic solid-phase extraction (MSPE) sorbents in analytical applications [11–14]. Yan et al. magnetized MIL-101 microcrystals by mixing MIL-101 with silica-coated Fe_3O_4 microparticles in an aqueous sample solution under sonication [11]. The hybridized sorbents were stabilized by static electronic interactions between the positively charged MIL-101 and the negatively charged Fe_3O_4 @ SiO_2 . Li and coworkers synthesized hybrid magnetic metal-organic framework-5 by a chemical bonding approach [12]. Chen et al. utilized Fe_3O_4 @MOF core-shell magnetic microspheres for MSPE of polychlorinated biphenyls from environmental water samples [14].

The sulfonamide antibiotics (SAs) are of toxic, anaphylactic, and carcinogenic characteristics

[15]. SAs assay is a crucial matter due to the worldwide emergence of these compounds in surface water, groundwater, and even drinking water [16]. The development of various sorbents for effective pre-concentration and separation of SAs by SPE has been actively pursued [17–20].

In this paper, $\text{Fe}_3\text{O}_4@\text{SiO}_2@\text{Fe-pamoate}$ was fabricated by assembly of Fe-pamoate porous complex onto the surface of silica-coated Fe_3O_4 NPs and its capability for extraction and separation of pollutants from environmental water sample was evaluated by using five types of SAs as model analytes. The assay of the target compounds was performed using high performance liquid chromatography (HPLC).

2. Experimental

2.1. Materials

Sodium acetate, $\text{FeCl}_3 \cdot 6\text{H}_2\text{O}$, ethylene glycol, poly(ethylene glycol) ($M_w=2000$), alcohol, acetone, acetic acid, aqueous ammonia solution, toluene, and *N,N*-dimethylformamide (DMF) were purchased from Sinopharm Chemical Reagent Co., Ltd., (Shanghai, China). Acetonitrile (ACN) was bought from Spectrum Chemical Mfg. Corp., (Shanghai, China). Tetraethyl orthosilicate (TEOS), 3-aminopropyltrimethoxysilane (APTES), succinic anhydride (SA), and 4-dimethylaminopyridine (DMAP) were obtained from Aladdin Chemical Reagent Co., (Shanghai, China). Pamoic acid was obtained from Sigma-Aldrich. All reagents were analytical grade.

Sulfadiazine (SDZ), sulfamerazine (SMR), sulfadimidine (SDD), sulfisoxazole (SIZ), and sulfathiazole (STZ) were purchased from J&K (Beijing, China) and their chemical structures are shown in Fig. 1. Individual stock solutions of the five SAs were prepared by dissolving 5.0 mg of the pure analytical standards in 10.0 mL of ACN. For the experiments, a working standard solution was prepared by deionized water to obtain the desired concentrations. All solutions were stored at 4 °C in the dark. The water samples were tap water, river water, and rain water. After sampling, the samples were transported to the laboratory immediately and stored in a refrigerator at 4 °C before use.

2.2. Synthesis of $\text{Fe}_3\text{O}_4@\text{SiO}_2$

Monodisperse magnetite (Fe_3O_4) was produced using a solvothermal method, as described in the literature [21]. The silica-coated magnetic particles were synthesized by suspending magnetic particles (0.2 g) in an ethanol/water (5:1 v/v) solution and adding ammonia solution (2 mL),

1
2
3 followed by dropwise addition of TEOS (1 mL) and sonication for 5 h at 40 °C. The obtained
4
5 $\text{Fe}_3\text{O}_4@\text{SiO}_2$ particles were separated from the solution using a permanent magnet, and washed three
6
7 times with ethanol and water, respectively.
8

9 **2.3. Synthesis of functionalized $\text{Fe}_3\text{O}_4@\text{SiO}_2$**

10
11 The nanoparticles were surface-modified to serve as a substrate for a step-by-step assembly by
12
13 treating the silica coated particles with an amino-functionalized silane, as described by Lelong et al.
14
15 [22]. $\text{Fe}_3\text{O}_4@\text{SiO}_2$ (0.05 g) was dispersed in toluene (50 mL) by ultrasonication and APTES (4 mL)
16
17 was added dropwise, and the mixture was refluxed at 110 °C with continuous stirring for 24 h. The
18
19 resulting functionalized $\text{Fe}_3\text{O}_4@\text{SiO}_2$ composites were recovered using a magnet, followed by
20
21 washing with ethanol and acetone several times, respectively. The particle surfaces were then
22
23 activated with succinic anhydride to introduce carboxyl groups. The amino-functionalized particles
24
25 (50 mg) were dispersed in absolute ethanol (100 mL) using sonication, and succinic anhydride (150
26
27 mg) and DMAP (300 mg) were added. The mixture was stirred for 8 h at 40 °C. Finally, the particles
28
29 were washed three times with ethanol.

30 **2.4. Synthesis of Fe-pamoate thin layers on pre-treated particles**

31
32 The functionalized particles (50 mg) were dispersed in $\text{FeCl}_3 \cdot 6\text{H}_2\text{O}$ in DMF/water (3:1, v/v)
33
34 solution (5 mL, 10 mM) for 15 min in an ultrasonic device. The particles were then magnetically
35
36 separated and washed with DMF (2 mL). Pamoic acid in DMF/water (3:1, v/v) solution (5 mL, 1
37
38 mM) was then added, and the mixture was kept in the ultrasonic device for 30 min. The particles
39
40 were then separated magnetically and washed with DMF (2 mL). After 20 cycles, the particles were
41
42 washed three times with DMF and dried under vacuum at 120 °C [10].

43 **2.5. Instruments**

44
45 Fourier transform infrared spectra (FT-IR) were acquired in the 400–4000 cm^{-1} region with an
46
47 EQUINX 55 FTIR spectrometer (Bruker Inc., Germany) using KBr pellets. Transmission electron
48
49 microscopy (TEM) images were obtained using a JEM-2100F microscope (JEOL, Japan).
50
51 Thermogravimetric analysis (TGA) was performed from room temperature to 600 °C at a ramp rate
52
53 of 10 °C min^{-1} using a Q600SDT thermal gravimetric analyzer (USA). The Brunauer-Emmett-Teller
54
55 (BET) surface area was measured in the $0.0 \leq P/P_0 \leq 1.0$ range with an ASAP 2020M micropore
56
57 physisorption analyzer (Micromeritics, Norcross, GA, USA) using nitrogen adsorption at 77 K. The
58
59
60

1
2
3 magnetic properties were measured at room temperature under a varying magnetic field from -20000
4 to 20000 Oe on a PMS-XL-7 superconducting quantum interference magnetic measurement system
5 (Quantum Design, USA). The concentration of Fe (III) ions was measured on ZA3000 atomic
6 absorption spectrophotometer (Hitachi, Japan).
7
8
9

10 11 **2.6. Chromatographic conditions**

12
13 HPLC analyses were performed using a Waters 1525 liquid chromatograph (Waters, USA). The
14 column compartment was maintained at 25 °C. Separation was performed using an Agilent TC-C₁₈
15 (2) column (4.6 × 250 mm, 5 μm). Mobile phase A comprised 0.1% (v/v) formic acid in acetonitrile
16 and mobile phase B comprised 0.1% (v/v) formic acid in Milli-Q water. Gradient elution with mobile
17 phase A was carried out as follows: 15% to 35% over 20 min, maintained for 5 min, and then back to
18 15% in 2 min, held for 5 min to equilibrate the column. The flow rate of the mobile phase was
19 maintained at 1.0 mL min⁻¹, the injection volume was 20 μL, and the ultraviolet detection
20 wavelength was 263 nm.
21
22
23
24
25
26
27

28 **2.7. Extraction procedure**

29
30 All extraction experiments were conducted in 20 mL glass vials. The sample solution (5 mL) was
31 placed in a glass vial containing Fe₃O₄@SiO₂@Fe-pamoate microspheres. The resulting solution
32 was sonicated for 2 min to disperse the microspheres, and then shaken vigorously for some time. An
33 external magnet was then placed beside the glass vial to separate the sorbents. The aqueous solution
34 was removed and acetone containing 0.5% aqueous ammonia (1 mL) was added to the vial as an
35 eluent for desorption of the adsorbate, the mixture was sonicated for 5 min and the desorption
36 procedure was repeated three times. The collected eluate was evaporated to dryness at 37 °C using a
37 concentrator. The obtained target was dissolved to 100 μL with acetonitrile, and 20 μL aliquot was
38 used for HPLC analysis.
39
40
41
42
43
44
45
46
47

48 **3. Results and discussion**

49 **3.1. Characterization of magnetic composite microspheres**

50
51 Formation of the ternary Fe₃O₄@SiO₂@Fe-pamoate single core-double shell structures involved
52 a three-step process, which is schematically illustrated in Fig. 2. First, Fe₃O₄@SiO₂ composite
53 microspheres with defined core-shell structures were obtained through a simple sol-process.
54
55
56
57
58
59
60

1
2
3 Subsequently, the $\text{Fe}_3\text{O}_4@\text{SiO}_2$ composite microspheres were functionalized with carboxyl groups.
4
5 Finally, through a step-by-step approach based on liquid-phase epitaxy, Fe-pamoate layers were
6
7 grown on the surface of the $\text{Fe}_3\text{O}_4@\text{SiO}_2$ composite microspheres to generate the ternary
8
9 $\text{Fe}_3\text{O}_4@\text{SiO}_2@\text{Fe-pamoate}$ single core-double shell structures.
10

11 The stages in the surface modification of $\text{Fe}_3\text{O}_4@\text{SiO}_2$ were also monitored systematically via
12 FT-IR spectroscopy (Fig. 3A). The bands at 1093 cm^{-1} and 806 cm^{-1} in the IR spectrum of
13 unmodified $\text{Fe}_3\text{O}_4@\text{SiO}_2$ are respectively assigned to the typical asymmetric stretching Si-O-Si and
14 symmetric stretching Si-O-Si bands of siliceous materials. The formation of $\text{Fe}_3\text{O}_4@\text{SiO}_2\text{-NH}_2$ was
15 confirmed by the presence of adsorption bands at 1497 cm^{-1} and 1564 cm^{-1} derived from the R-NH₂
16 groups, and the 2935 cm^{-1} peak can be assigned to the C-H stretching vibrations. The peak observed
17 at 1622 cm^{-1} after reaction with succinic anhydride can be assigned to the C=O vibrations [23]. Fig.
18 3B shows the FT-IR spectra of H₂pam and $\text{Fe}_3\text{O}_4@\text{SiO}_2@\text{Fe-pamoate}$. It is well known, the
19 absorption peaks of the carboxyl groups in the organic ligands are shifted to lower wave number
20 after complexation with metal ions. In the case of Fe-pamoate, the absorption peaks of the C=O
21 bond at 1691 cm^{-1} and the C-O bond at 1452 cm^{-1} in pamoic acid are shifted to 1636 cm^{-1} and 1382
22 cm^{-1} , which characterizes the carboxylate groups of the framework [24].
23
24
25
26
27
28
29
30
31
32
33

34 Typical TEM images of $\text{Fe}_3\text{O}_4@\text{SiO}_2$ and $\text{Fe}_3\text{O}_4@\text{SiO}_2@\text{Fe-pamoate}$ were shown in Fig. 3C and
35 Fig. 3D, respectively. From Fig. 3C, it can be seen that the dark magnetic particles were coated with
36 a uniform light-grey SiO_2 shell. After coating with a thin SiO_2 layer, the average diameter of the
37 $\text{Fe}_3\text{O}_4@\text{SiO}_2$ particles was 420 nm. Fig. 3D shows that the $\text{Fe}_3\text{O}_4@\text{SiO}_2@\text{Fe-pamoate}$ magnetic
38 microspheres is consist of a dark Fe_3O_4 core, a light-grey SiO_2 middle layer, and a grey Fe-pamoate
39 shell with a thickness of about 100 nm, clearly demonstrating the formation of a unique ternary
40 single core-double shell structure.
41
42
43
44
45
46

47 The porosity of the as-synthesized $\text{Fe}_3\text{O}_4@\text{SiO}_2@\text{Fe-pamoate}$ material was confirmed by
48 nitrogen sorption-desorption isotherms. Before assembly Fe-pamoate complexes, the specific surface
49 area of the $\text{Fe}_3\text{O}_4@\text{SiO}_2$ -carboxylated microspheres was approximately $8.6\text{ m}^2\text{ g}^{-1}$. After
50 step-by-step assembly (20 cycles) of Fe-pamoate complexes, the specific surface area of the
51 magnetic microspheres was increased to $173.91\text{ m}^2\text{ g}^{-1}$ (Fig. 4A). Thus, the specific surface area of
52 $\text{Fe}_3\text{O}_4@\text{SiO}_2@\text{Fe-pamoate}$ was derived mainly from the Fe-pamoate layers.
53
54
55
56
57
58
59
60

1
2
3 The thermal stability of the $\text{Fe}_3\text{O}_4@\text{SiO}_2@\text{Fe-pamoate}$ particles was shown in Fig. 4B. A weight
4 loss of about 2% was observed in the temperature range of 23–158 ° C, this loss might be due to
5 the evacuation of one non-coordinated DMF and one water molecule from the framework. The
6 weight remained constant between 158 and 210 ° C, a weight loss of ~10% at 300 °C, which
7 indicated decomposition of the overall structure. In addition, the stability of the
8 $\text{Fe}_3\text{O}_4@\text{SiO}_2@\text{Fe-pamoate}$ in different pH and different solvent was measured by detecting the
9 concentration of Fe (III) ions released from the Fe-pamoate skeleton disruption. Fig 4C shows that
10 the concentrations of Fe (III) ions were not detected in solution at pH greater than 5, and could be
11 detected at pH 2-5, which indicated that the framework of $\text{Fe}_3\text{O}_4@\text{SiO}_2@\text{Fe-pamoate}$ is unstable at
12 acidic conditions. Fe (III) ions were not detected in different solvents (methanol, acetonitrile,
13 acetone), which suggested that the $\text{Fe}_3\text{O}_4@\text{SiO}_2@\text{Fe-pamoate}$ is stable in such three solvents.

14
15
16
17
18
19
20
21
22
23
24
25
26
27
28
29
30
31
32
33
34
35
36
37
38
39
40
41
42
43
44
45
46
47
48
49
50
51
52
53
54
55
56
57
58
59
60
The magnetization curve was shown in Fig. 4D. The $\text{Fe}_3\text{O}_4@\text{SiO}_2@\text{Fe-pamoate}$ microspheres
exhibited typical superparamagnetic behavior and had magnetic saturation (MS) value of about 6.59
emu g⁻¹. In addition, after dispersing in water, the magnetic particles could be collected using a
magnet within 30 s, which indicated that the magnetic microspheres could be used for magnetic
separation.

3.2. Optimization of extraction conditions

The procedure for SAs extraction was optimized by evaluating several parameters, i.e., the
amount of the adsorbent, extraction time, desorption solvent, and pH of the sample solution. The
chromatographic peak area, which is related to the number of moles of analyte extracted, was used to
evaluate the efficiency of extraction of the target analytes by the microspheres under different
experimental conditions.

3.2.1 Effect of the amount of adsorbent on extraction efficiency

The effect of the amount of the magnetic $\text{Fe}_3\text{O}_4@\text{SiO}_2@\text{Fe-pamoate}$ particles on the extraction
efficiency was investigated with 3 to 25 mg of magnetic particles in a 5 mL aqueous solution spiked
and the results were shown in Fig. 5A. The peak areas of the analytes were first increased with
adsorbent amount increasing from 3 to 10 mg and then no significant increase was observed. Hence,
10 mg of $\text{Fe}_3\text{O}_4@\text{SiO}_2@\text{Fe-pamoate}$ was selected as the amount of adsorbent. Furthermore, the
extraction efficiencies of $\text{Fe}_3\text{O}_4@\text{SiO}_2@\text{Fe-pamoate}$ particles were compared with those of

1
2
3 Fe₃O₄@SiO₂ particles (Fig 5A). The results showed that Fe₃O₄@SiO₂@Fe-pamoate gave much
4
5 larger extraction efficiency than the Fe₃O₄@SiO₂, which demonstrated the extraction capacity for
6
7 SAs was mainly derived from the Fe-pamoate layers.

9 3.2.2. Effect of extraction time on extraction efficiency

10
11 The extraction time is a very important parameter, which affects the partition of the target
12
13 analytes between the sample solution and adsorbent. The effect of the extraction time on the
14
15 efficiency of extraction of the target analytes from the aqueous medium using the microspheres was
16
17 evaluated over the course of 5–150 min using a deionized aqueous sample. The results shown in Fig.
18
19 5B, the extraction efficiency rapid increased when extraction time from 5-30 min and then had no
20
21 significant change. The adsorbent possessed a thicker adsorption layer (about 100 nm), and
22
23 sulfonamide antibiotics molecules were needed time entering the adsorption layer and deep pore. As
24
25 a compromise of save time and good extraction efficiency, 30 min was chosen as the extraction time.

26 3.2.3. Effect of pH on extraction efficiency

27
28 The adsorption of the five SAs on Fe₃O₄@SiO₂@Fe-pamoate was significantly pH dependent
29
30 (Fig. 5C). The highest extraction efficiency for all five SAs was obtained at pH 6.0, and then
31
32 declined gradually as the pH was either increased to 8.0 or decreased to 2.0. The pH of the solution
33
34 may affect the speciation of the SAs as well as the structure of Fe₃O₄@SiO₂@Fe-pamoate. At pH
35
36 values below 6.0, the structure of Fe-pamoate was destroyed in the acidic medium. Thus, the
37
38 adsorption of the SAs was reduced with pH being decreased. At pH 6, the SAs are predominantly in
39
40 the neutral form (SAs⁰), thus hydrogen bonding between the N-containing groups of SAs⁰ and the
41
42 surface -OH of Fe₃O₄@SiO₂@Fe-pamoate and π - π electron coupling were the major driving forces
43
44 for adsorption. Increasing the pH from 7.0 to 8.0, more neutral molecules (SAs⁰) were transformed
45
46 to the anionic form (SAs⁻). Hence, the resultant weakening of the hydrogen bonds and suppression
47
48 of π - π electron coupling could strongly impair the adsorption process [26]. For the ensuing further
49
50 studies, the sample solution was adjusted to pH 6.0 to achieve the highest extraction efficiency.

51 3.2.4. Effect of desorption solvent

52
53 After extraction, the analytes were desorbed from the adsorbent with an organic solvent and
54
55 analysed via HPLC. Three organic solvent mixtures, i.e., MeOH containing 0.5% ammonium
56
57 hydroxide, ACN containing 0.5% ammonium hydroxide, and acetone containing 0.5% ammonium
58
59

hydroxide, were evaluated to identify the optimum desorption solvent [25]. The highest extraction efficiency was achieved with acetone containing 0.5% ammonium hydroxide based on the HPLC results (Fig. 5D).

3.3. Method validation

The optimized MSPE-HPLC-UV method employing $\text{Fe}_3\text{O}_4@\text{SiO}_2@\text{Fe-pamoate}$ magnetic microspheres was validated as summarized in Table 1. The response linearity of the technique was measured by extracting a series of standard solutions containing all five SAs. The correlation coefficients (R^2) were between 0.9947 and 0.9988. The limits of detection (LODs) based on a signal-to-noise ratio of 3 were within the range of 0.08–0.12 ng mL^{-1} , and the limits of quantification (LOQs) based on a signal-to-noise ratio of 10 were within the range of 0.26–0.40 ng mL^{-1} . Thus, the MSPE technique using $\text{Fe}_3\text{O}_4@\text{SiO}_2@\text{Fe-pamoate}$ magnetic microspheres coupled with UV detection offered the merits of excellent sensitivity, simplicity, and operational ease.

3.4. Sample analysis

The proposed method was used for the determination of SAs in tap water, river water, and rain water samples. No SAs were detected in these environmental water samples. To further validate the established method, the recoveries were determined for spiked environmental samples at three levels, i.e., 3, 10, and 30 ng mL^{-1} . Chromatograms of the blank water sample, water sample spiked 10 ng mL^{-1} of the analytes, and the extracted solution were shown in Fig. 6. No peaks corresponding to the five SAs appeared for blank water sample. The intensity of the peaks was very low for the water samples spiked with SAs at a level of 10 ng mL^{-1} , whereas the intensity of these peaks increased significantly after extraction using the $\text{Fe}_3\text{O}_4@\text{SiO}_2@\text{Fe-pamoate}$ microspheres. The recovery ratio of the five SAs in the tap water, river water, and rain water samples were 88.3–98.9%, 86.3–99.7%, and 89.5–97.2%, respectively, as shown in Table 2. These results indicated that the proposed method is applicable for extraction of trace sulfonamides in complex environmental water samples.

4. Conclusion

$\text{Fe}_3\text{O}_4@\text{SiO}_2@\text{Fe-pamoate}$ microspheres were successfully synthesized via a step-by-step assembly strategy. The microspheres consisted of a magnetic core, a SiO_2 middle layer, and a

1
2
3 Fe-pamoate complex shell, and were utilized as adsorbents for the extraction and enrichment of SAs
4 in water samples. Strong π - π electron coupling and hydrogen bonding between Fe-pamoate and the
5 analytes enabled extraction and enrichment of the SAs with high efficiency. Furthermore, the
6 magnetic property of the Fe_3O_4 core facilitated easy separation of the sorbent from the water sample
7 and eluent. The proposed procedure based on $\text{Fe}_3\text{O}_4@ \text{SiO}_2@ \text{Fe-pamoate}$ microspheres offers the
8 merits of speed, simplicity, and convenience for assay of SAs in environmental water samples, and
9 the method is prospectively applicable for the detection of other compounds.
10
11
12
13
14
15
16

17 **Acknowledgments**

18
19
20 The project was supported by National Natural Science Foundation of China (No. 21275098) and
21 Doctor Base Foundation of Chinese Ministry of Education (No. 20110202110005).
22
23
24
25
26
27
28
29
30
31
32
33
34
35
36
37
38
39
40
41
42
43
44
45
46
47
48
49
50
51
52
53
54
55
56
57
58
59
60

References

- [1] L. H. Reddy, J. L. Arias, J. Nicolas and P. Couvreur, *Chem. Rev.*, 2012, 112, 5818–5878.
- [2] J. P. Ge, Y. X. Hu, M. Basin, W. P. Dobermann and Y. D. Yin, *Agnew. Chem. Int. Ed.*, 2007, 46, 4342–4345.
- [3] H. Lee, E. Lee, D. K. Kim, N. K. Jang, Y. Y. Jeong and S. Y. Jon, *J. Am. Chem. Soc.*, 2006, 128, 7383–7389.
- [4] M. Arruebo, M. Galán, N. Navascués, C. Téllez, C. Marquina, M. R. Ibarra and J. Santamaría, *Chem. Mater.*, 2006, 18, 1911–1919.
- [5] Y. H. Deng, C. H. Deng, D. W. Qi, C. Liu, J. Liu, X. M. Zhang and D. Y. Zhao, *Adv. Mater.*, 2009, 21, 1377–1382.
- [6] L. Wang, X. H. Zang, Q. Y. Chang, C. Wang and Z. Wang, *Anal. Methods*, 2014, 6, 253–260.
- [7] R. Shen, F. Yang, J. Q. Wang, Y. Li, S. J. Xie, C. Y. Chen, Q. Y. Cai and S. Z. Yao, *Anal. Methods*, 2011, 3, 2909–2914.
- [8] L. R. Kong, X. F. Lu, X. J. Bian, W. J. Zhang and C. Wang, *ACS Appl. Mater. Inter.*, 2011, 3, 35–42.
- [9] M. E. Silvestre, M. Franzreb, P. G. Weidler, O. Shekhah and C. Wöll, *Adv. Funct. Mater.*, 2013, 23, 1210–1213.
- [10] F. Ke, L. G. Qiu, Y. P. Yuan, X. Jiang and J. F. Zhu, *J. Mater. Chem.*, 2012, 22, 9497–9500.
- [11] S. H. Huo and X. P. Yan, *Analyst*, 2012, 137, 3445–3451.
- [12] Y. L. Hu, Z. L. Huang, J. Liao and G. K. Li, *Anal. Chem.*, 2013, 85, 6885–6893.
- [13] S. L. Zhang, Z. Jiao, W. X. Yao, *J. Chromatogr., A*, 2014, 1371, 74–81.
- [14] X. F. Chen, N. Ding, H. Zang, H. Yeung, R. S. Zhao, C. G. Cheng, J. H. Liu and T. W. D. Chan, *J. Chromatogr., A*, 2013, 1304, 241–245.
- [15] C. Accinelli, W. C. Koskinken, J. M. Becker and M. J. Sadowsky, *J. Agric. Food Chem.*, 2007, 55, 2677–2682.
- [16] A. Boxall, D. Kolpin, B. Holling-Sorensen and J. Tolls, *Environ. Sci. Technol.*, 2003, 37 (15), 286A–294A.
- [17] S. L. Qin, S. Deng, L. Q. Su and P. Wang, *Anal. Methods*, 2012, 4, 2182–2188.

- 1
2
3 [18] Y. B. Luo, Z. G. Shi, Q. Gao and Y. Q. Feng, *J. Chromatogr., A*, 2011, 1218, 1353–1358.
4
5 [19] A. V. Herrera-Herrera, J. Hernández-Borges, M. M. Afonso, J. A. Palenzuela and M. A.
6
7 Rodríguez-Delgado, *Talanta*, 2013, 116, 695–703.
8
9 [20] X. L. Bao, Z. M. Qiang, J. H. Chang, W. W. Ben and J. H. Qu, *J. Environ. Sci.*, 2014, 26,
10
11 962–969.
12
13 [21] J. Liu, Z. K. Sun, Y. H. Deng, Y. Zou, C. Y. Li, X. H. Guo, L. Q. Xiong, Y. Gao, F. Y. Li and D.
14
15 Y. Zhao, *Angew. Chem. Int. Ed.*, 2009, 48, 5875–5879.
16
17 [22] Q. Yuan, N. Li, Y. Ci, C. W. Geng, W. F. Yan, Y. Zhao, X. T. Li and B. Dong, *J. Hazard. Mater.*,
18
19 2013, 254, 157–165.
20
21 [23] A. Suwalski, H. Dabboue, A. Delalande, S. F. Bensamoun, F. Canon, P. Midoux, G. Saillant, D.
22
23 Klatzmann, J. P. Salvetat and C. Pichon, *Biomaterials*, 2010, 31, 5237–5245.
24
25 [24] A. Vimont, J. M. Goupil, J. C. Lavalley, M. Daturi, S. Surblé, C. Serre, F. Millange, G. Férey,
26
27 and N. Audebrand, *J. Am. Chem. Soc.*, 2006, 128, 3218–3227.
28
29 [25] M. Seifrtová, L. Nováková, C. Lino, A. Pena and P. Solich, *Anal. Chim. Acta*, 2009, 649,
30
31 158–179.
32
33 [26] Z. Hasan and S. H. Jhung, *J. Hazard. Mater.*, 2015, 283, 329–339.
34
35
36
37
38
39
40
41
42
43
44
45
46
47
48
49
50
51
52
53
54
55
56
57
58
59
60

Figure captions

Fig. 1 Chemical structures of SAs used in this work

Fig. 2 Schematic illustration of the process of $\text{Fe}_3\text{O}_4@\text{SiO}_2@\text{Fe-pamoate}$ single core-double shell sandwich structure formation

Fig. 3 (A) FT-IR absorbance spectra of $\text{Fe}_3\text{O}_4@\text{SiO}_2$ (a), $\text{Fe}_3\text{O}_4@\text{SiO}_2\text{-NH}_2$ (b) and $\text{Fe}_3\text{O}_4@\text{SiO}_2\text{-COOH}$ (c); (B) FT-IR spectra of H_2pam (a) and $\text{Fe}_3\text{O}_4@\text{SiO}_2@\text{Fe-pamoate}$ (b); and TEM images of (C) $\text{Fe}_3\text{O}_4@\text{SiO}_2$ and (D) $\text{Fe}_3\text{O}_4@\text{SiO}_2@\text{Fe-pamoate}$.

Fig. 4 (A) Nitrogen sorption-desorption isotherms of magnetic $\text{Fe}_3\text{O}_4@\text{SiO}_2@\text{Fe-pamoate}$, the inset shows the corresponding pore size distribution analysis; (B) TGA curve of $\text{Fe}_3\text{O}_4@\text{SiO}_2@\text{Fe-pamoate}$ acquired under air; (C) The concentration of Fe (III) detected at different pH; and (D) Room-temperature magnetization curve of $\text{Fe}_3\text{O}_4@\text{SiO}_2@\text{Fe-pamoate}$.

Fig. 5 Effects of experimental conditions on the extraction and desorption of five SAs. (A) Amount of adsorbent (the inset shows the comparison of $\text{Fe}_3\text{O}_4@\text{SiO}_2@\text{Fe-pamoate}$ with $\text{Fe}_3\text{O}_4@\text{SiO}_2$), (B) extraction time, (C) pH of the solution, and (D) desorption solvent.

Fig. 6 HPLC-UV chromatograms of (A) tap water sample, (B) river water sample, (C) rain water sample. (a) and (b) before and after spiking with 10 ng mL^{-1} of each compound, and (c) after extraction of 10 ng mL^{-1} spiked sample using magnetic microspheres; (1) SDZ, (2) STZ, (3) SMR, (4) SDD and (5) SIZ.

Table 1

Linear ranges, regression data, limits of detection (LOD), and limits of quantification (LOQ) for determination of SAs

SAs	Linear range (ng mL ⁻¹)	Calibration curves			LOD (ng mL ⁻¹)	LOQ (ng mL ⁻¹)
		Slope	Intercept	<i>R</i> ²		
SDZ	0.5–50	5830.4	-1095.3	0.9984	0.08	0.26
SMR	0.5–50	49417	56823	0.9947	0.09	0.30
SDD	0.5–50	58968	-36431	0.9988	0.12	0.40
SIZ	0.5–50	7817.5	38139	0.9988	0.10	0.34
STZ	0.5–50	70541	-48287	0.9979	0.10	0.33

Table 2 Determination of the five SAs and recoveries in environmental water sample

SAs	Spiking level (ng mL ⁻¹)	Mean recovery (% , n = 3)		
		Tap water	River water	Rain water
	0.0	nd ^a	nd	nd
SDZ	3.0	90.4 ± 2.4	94.1 ± 11.7	89.5 ± 4.8
	10.0	93.3 ± 3.1	96.5 ± 7.3	90.5 ± 3.7
	30.0	95.5 ± 5.7	97.6 ± 10.6	97.2 ± 2.7
SMR	0.0	nd	nd	nd
	3.0	91.6 ± 7.6	92.4 ± 8.6	89.6 ± 6.4
	10.0	94.6 ± 3.4	94.6 ± 8.5	95.4 ± 1.8
SDD	30.0	97.2 ± 8.4	98.3 ± 7.6	96.2 ± 5.9
	0.0	nd	nd	nd
	3.0	88.3 ± 12.3	93.7 ± 4.7	92.3 ± 8.6
SIZ	10.0	92.7 ± 1.4	97.8 ± 4.4	92.6 ± 10.1
	30.0	96.0 ± 6.5	99.7 ± 6.9	95.7 ± 7.4
	0.0	nd	nd	nd
STZ	3.0	93.1 ± 4.7	86.2 ± 8.2	92.5 ± 6.9
	10.0	97.0 ± 6.3	97.5 ± 2.9	95.3 ± 3.5
	30.0	97.6 ± 8.9	98.2 ± 8.7	97.0 ± 3.3
	0.0	nd	nd	nd
	3.0	90.4 ± 9.0	92.7 ± 9.7	89.5 ± 8.3
	10.0	95.1 ± 3.0	94.5 ± 5.9	92.7 ± 6.1
	30.0	98.9 ± 5.4	96.5 ± 11.5	96.7 ± 7.4

^a nd: not detected

Fig. 1

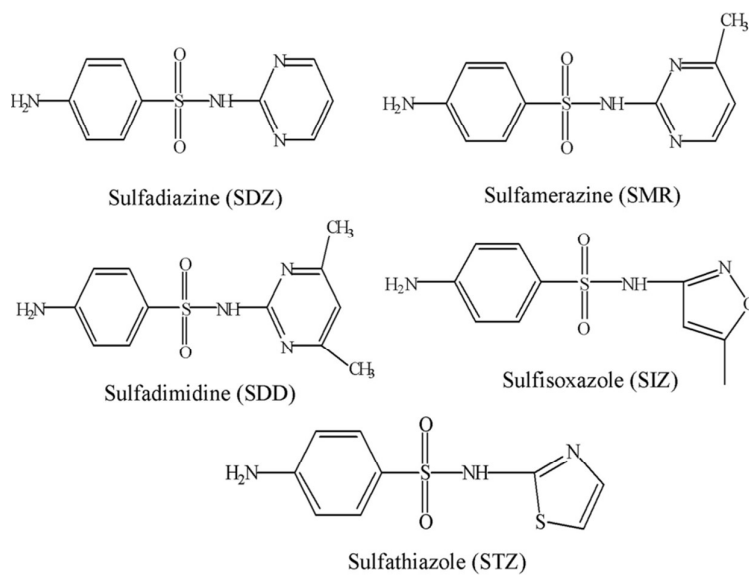


Fig. 2

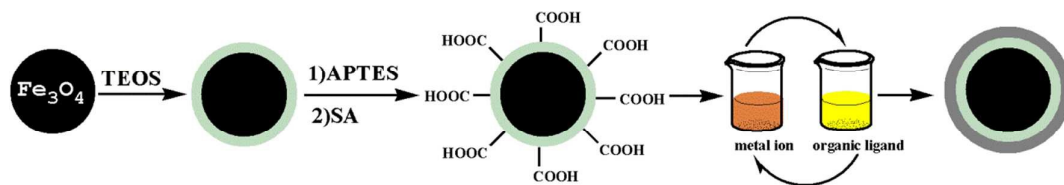


Fig. 3

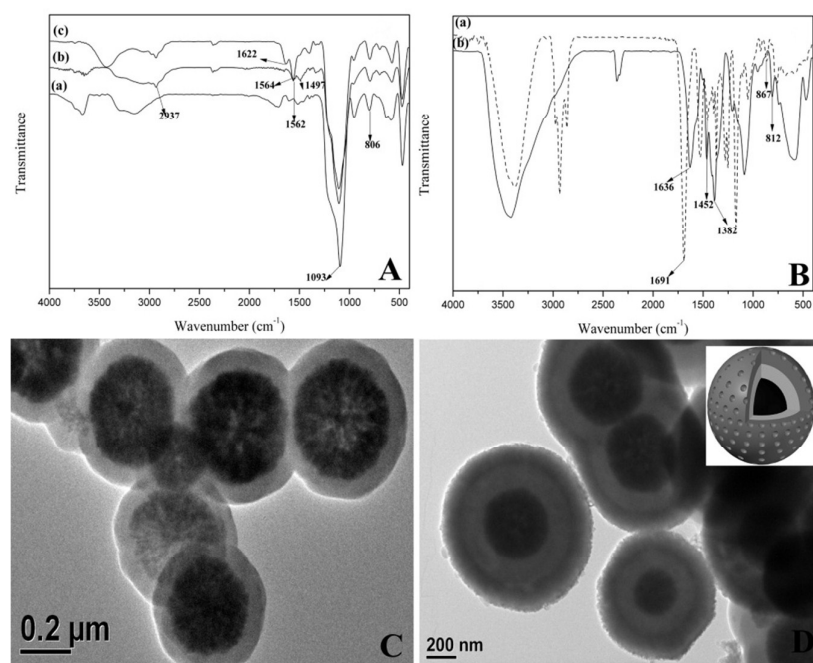


Fig. 4

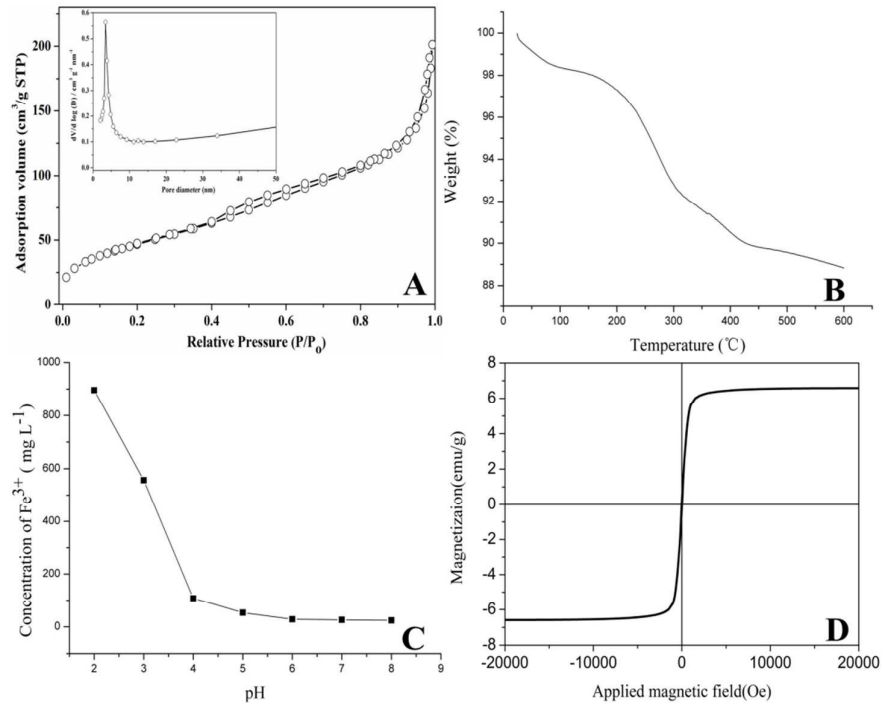
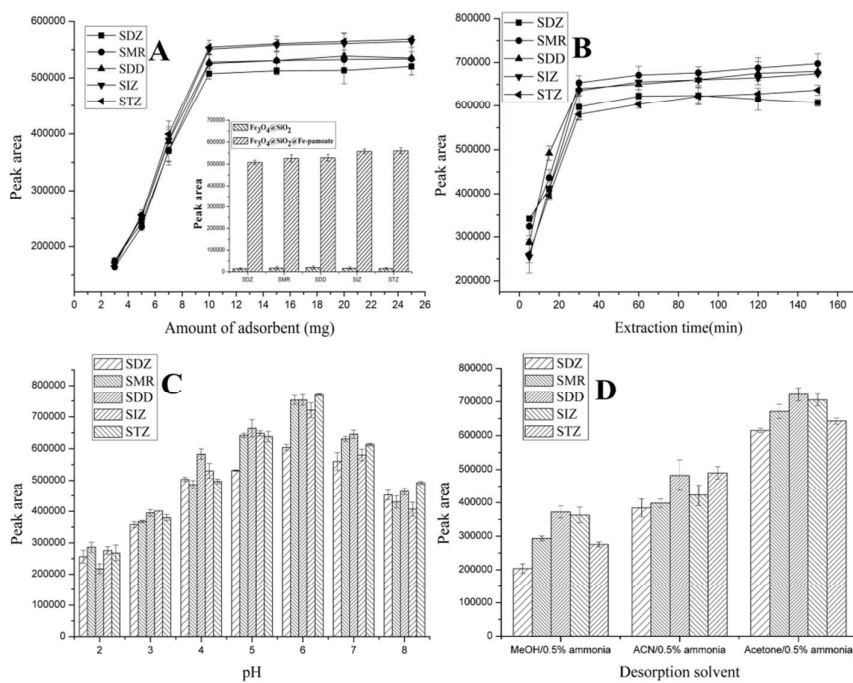


Fig. 5



Analytical Methods Accepted Manuscript

Fig. 6

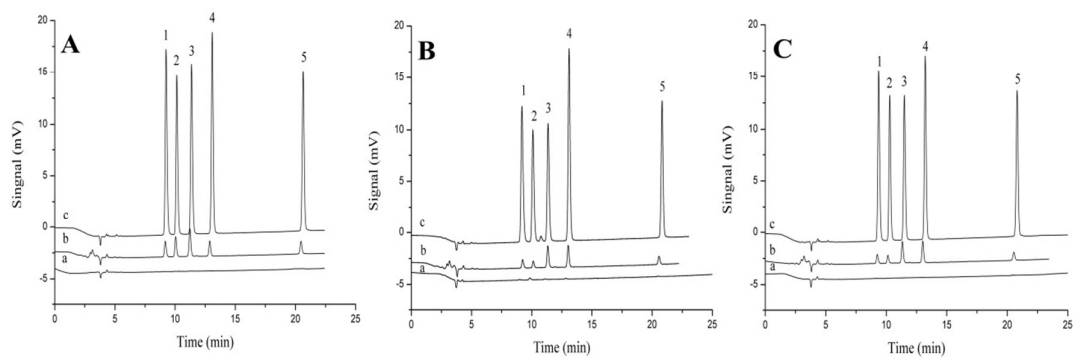
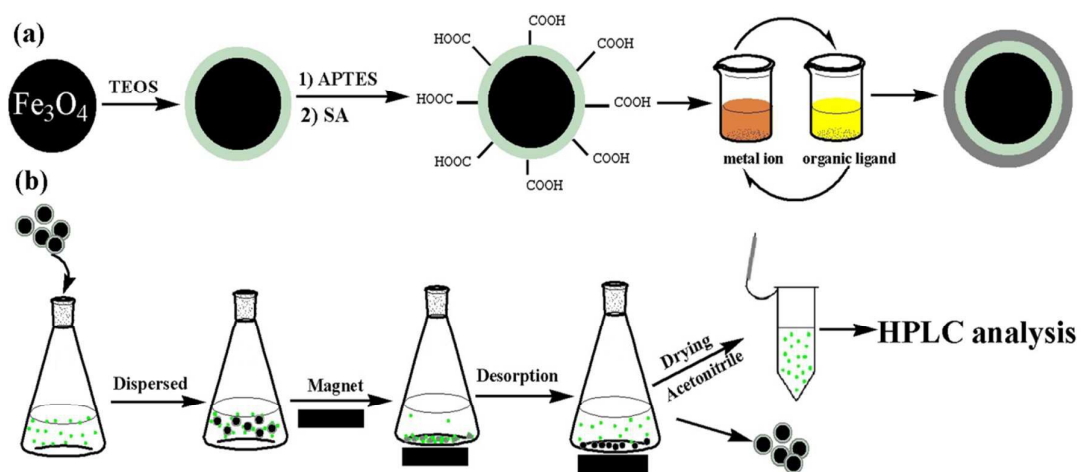


Table of contents entry



$\text{Fe}_3\text{O}_4@SiO_2@Fe\text{-pamoate}$ single core-double shell microspheres have been synthesized via step-by-step assembly strategy and were used to extract sulfonamide antibiotics